AEA FUS 255

AEA Technology
Fusion
(UKAEA/Euratom Fusion Association)

The Excitation of Obliquely Propagating Fast Alfven Waves at Fusion Ion Cyclotron Harmonics

R O Dendy, C N Lashmoor-Davies,
K G McClements and G A Cottrell

November 1993

AEA Technology
Fusion

Culham, Abingdon
Oxfordshire OX14 3DB
United Kingdom
Telephone 0235 463377
Facsimile 0235 463647

The Excitation of Obliquely Propagating Fast Alfvén Waves at Fusion Ion Cyclotron Harmonics

R.O. Dendy, C.N. Lashmore-Davies, and K.G. McClements

AEA Technology, Fusion, Culham, Abingdon, Oxfordshire, OX14 3DB, UK
(Euratom/UKAEA Fusion Association)

G.A. Cottrell

JET Joint Undertaking, Abingdon, Oxfordshire, OX14 3EA, UK

ABSTRACT

The theory of the magnetoacoustic cyclotron instability, which has been proposed as a mechanism for suprathermal ion cyclotron harmonic emission observed in large tokamaks, is generalized to include finite parallel wavenumber $k_{\parallel}$. This extension introduces significant new physics: the obliquely propagating fast Alfvén wave can undergo cyclotron resonant interactions with thermal and fusion ions, which affects the instability driving and damping mechanisms. The velocity-space distribution of the fusion ions is modelled by a drifting ring, which approximates the distribution calculated for the emitting region in tritium experiments on the Joint European Torus (JET) [Cottrell et al., Nucl. Fusion, in press (1993)]. Linear instability can occur simultaneously at the fusion ion cyclotron frequency and all its harmonics when the fusion ion concentration is extremely low, because the finite $k_{\parallel}$ gives rise to a Doppler shift which decouples cyclotron damping due to thermal ions from wave growth associated with fusion ions. Doppler shifts associated with finite $k_{\parallel}$ may also be related to the observed splitting of harmonic emission lines.

PACS numbers: 52.25Sw, 52.35Qz, 52.35Hr, 52.55Pi

I. INTRODUCTION

There are strong observational links between ion cyclotron emission (ICE) and fusion reactivity in tokamak plasmas. These links originally emerged from ohmic deuterium discharges in the Joint European Torus (JET)[1–3] and the Tokamak Fusion Test Reactor (TFTR),[4] and were demonstrated most recently in the Preliminary Tritium Experiment on JET.[5–7]. They include: the proportionality of ICE intensity to measured fusion reactivity over a range of six decades in signal intensity; correlations in the time–evolution of the ICE signal and neutron flux during discharges; the matching of ICE spectral peak frequencies to successive local ion cyclotron harmonics at the outer mid–plane edge; and correlations between ICE and the observed impact of MHD activity, such as sawteeth and ELMs, on energetic ions. A detailed review of many of the observational features of ICE is given in Ref. 8. The potential of ICE as a diagnostic of fusion product populations in tokamak plasmas is, accordingly, widely recognized. However, its exploitation will require a full understanding of the physics of the underlying emission mechanism.

The magnetoacoustic cyclotron instability[9–11] is a strong candidate emission mechanism for ICE: it belongs to a family of high frequency energetic ion–driven collective instabilities which have been studied over the past three decades.[12–16] The theory of the magnetoacoustic cyclotron instability was first developed in detail in Ref. 9, where the excitation of perpendicular–propagating waves on the fast Alfvén and ion Bernstein branches was shown to be possible at frequencies close to the cyclotron harmonics $\ell\Omega_\alpha$ of an energetic ion species α displaying some form of population inversion in velocity–space. In Ref. 9, the crucial role of cyclotron harmonic (Bernstein) waves supported by the majority thermal ion population i was also recognized: the most nearly resonant such wave ($s\Omega_i \simeq \ell\Omega_\alpha$) provides positive–energy loading which determines the threshold of the instability. The analysis presented in Ref. 9, which was restricted to frequencies $\omega \gg \Omega_i$, was extended in Refs. 10 and 11 to the frequency range $\omega \sim \Omega_i$ required for application to early JET ICE results. It was shown that the perpendicular magnetoacoustic cyclotron instability had properties broadly consistent with those required for an ICE emission mechanism, in the appropriate parameter range. We note that this instability appears also to provide a viable emission mechanism for signals detected near the Earth's plasmapause[17] and bow shock.[18] For an early review of the potential role of this class of instability in tokamak reactors, see Ref. 19.

In the present paper we generalize the theory of the magnetoacoustic cyclotron instability to include oblique propagation. This means that we must consider wave–particle resonant cyclotron damping, in addition to the wave–wave resonant positive–energy loading mentioned above. We will show that, except for quasi–perpendicular propagation, cyclotron damping is in fact the dominant stabilization mechanism. Part of the motivation for extending the theory in this way lies in the fact that there remain several distinctive features of the ICE data which the strictly perpendicular magnetoacoustic cyclotron instability cannot easily account for. These include: the simultaneous excitation of all cyclotron harmonics from $\ell = 1$ upwards; the splitting of spectral peaks, noted in Refs. 5–7; and the excitation of proton half–harmonics in pure deuterium ohmic discharges.

In Sec. II we propose, on the basis of orbit calculations presented in Ref. 7, that the fusion ion distribution in the edge plasma of JET can be modelled as a drifting ring with a Maxwellian spread of velocities parallel to the magnetic field. The appropriate dispersion relation is derived in Sec. III, and a perturbative analysis of this dispersion relation is presented in Sec. IV. In Sec. V we present the results of a full numerical study of the magnetoacoustic cyclotron instability for oblique propagation. In Sec. V. we also discuss the significance of our results in relation to ICE data from JET, and in Sec. VI we briefly consider the problem of wave propagation. Our conclusions are presented in Sec. VII.

II. DISTRIBUTION OF FUSION IONS

The magnetoacoustic cyclotron instability is driven by the free energy associated with non–Maxwellian features in the velocity-space distribution of the energetic ion population.

Model distributions are typically chosen according to criteria that include applicability to specific physical scenarios and analytical tractability: for the case of perpendicular propagation, models have included shells,[9,10] extended shells,[11,20] and rings.[9,17] The underlying character of the instability, in terms of excitation of waves on the fast Alfvén–ion Bernstein branch at ion cyclotron harmonics, has remained broadly independent of the details of velocity–space structure.

In the present paper, where the primary emphasis is on the new physics introduced by the inclusion of finite parallel wavenumber, our choice for the model velocity–space distribution of the energetic ions is guided by the considerations outlined in Ref. 7. There, it was pointed out that the observed localization of the ICE emitting region to the outer mid–plane edge may be due primarily to the uniquely unstable character of the energetic ion velocity–space distribution within that region. It has been shown[7,21] that a certain subgroup of centrally born fusion ions, restricted to a specific narrow range of pitch–angles just inside the trapped–passing boundary, make large drift orbit excursions which carry them to the outer mid–plane edge. These particles are much more numerous than fusion ions born locally, and consequently dominate the fusion ion velocity distribution in the ICE emitting region. The maximum radial excursion varies as $\rho_\theta^{2/3}$, where ρ_θ is the poloidal Larmor radius. In the case of pure deuterium discharges, there are three charged products of primary fusion reactions: protons, tritons, and helium–3 nuclei. Of these, only protons and tritons have sufficiently large poloidal Larmor radii to undergo large excursion orbits from the centre of JET to the outer mid–plane edge. Centrally–born helium–3 nuclei cannot do so, and are therefore not expected to play any significant role in the generation of ICE in JET.[7] In this paper we are primarily concerned with the interpretation of data from the JET tritium experiment, in which the most abundant charged fusion products were alpha-particles.[7] For this reason, the numerical results presented in Sec. V were obtained for the case of an alpha-particle fusion ion population.

For reasons of analytical tractability, and following the spirit of Ref. 7, we adopt a model for the velocity-space distribution of fusion ions in the emitting region which has a drifting Maxwellian distribution of velocities parallel to the magnetic field, and a unique velocity perpendicular to the field. Normalized to unity, the fusion ion distribution is thus given by

$$f_\alpha = \frac{1}{2\pi^{3/2} u v_r} \exp\left(-\frac{(v_\parallel - v_d)^2}{v_r^2}\right) \delta(v_\perp - u), \tag{1}$$

where $v_\parallel$, $v_\perp$ denote velocity components parallel and perpendicular to the magnetic field, and u, v_d, v_r are parameters which define respectively the unique perpendicular speed, average parallel drift speed, and parallel velocity spread of the fusion ions. Typically $u^2 \gg v_d^2$, and fusion ions with energies significantly less than the birth energy do not reach the edge plasma.[7] The value of u is thus determined essentially by the birth energy.

As in previous papers,[10–11,17–18] we shall establish certain features of the magnetoacoustic cyclotron instability that are generic, and are not restricted by the particular choice of distribution function parameters.

III. DISPERSION RELATION FOR OBLIQUE PROPAGATION

We assume that the wave electric field is approximately polarized in the plane perpendicular to the magnetic field direction, z, so that electron Landau damping can be neglected. In such cases we only require the (x,x), (x,y) and (y,y) components of the dielectric tensor ϵ_{ij}. For a wave propagating in the (x,z) plane, the appropriate dispersion relation is

$$\left(\epsilon_{xx} - \frac{k_z^2 c^2}{\omega^2}\right)\left(\epsilon_{yy} - \frac{k^2 c^2}{\omega^2}\right) = -\epsilon_{xy}^2, \tag{2}$$

where ω is the complex wave frequency, $\mathbf{k} = (k_x, 0, k_z)$ is the wave vector and c is the speed of light. ϵ_{xx}, ϵ_{xy} and ϵ_{yy} contain contributions from both electrons and ions, but when ω is of the order of the ion cyclotron frequencies the electron contribution to ϵ_{xx} is negligibly small.[9] In this frequency régime we can write

$$\epsilon_{xx} = \epsilon_{xx}^i + \epsilon_{xx}^\alpha, \tag{3}$$

$$\epsilon_{xy} = \epsilon^e_{xy} + \epsilon^i_{xy} + \epsilon^\alpha_{xy}, \tag{4}$$

$$\epsilon_{yy} = \epsilon^e_{yy} + \epsilon^i_{yy} + \epsilon^\alpha_{yy}. \tag{5}$$

In the above expressions the superscripts e, i and α refer to electrons, bulk ions, and fusion ions respectively. If $\omega \ll \Omega_e$, and $z_e^2 \equiv k_x^2 v_e^2/2\Omega_e^2 \ll 1$, where v_e is the electron thermal speed, we can write

$$\epsilon^e_{xy} = -i\frac{\omega_{pe}^2}{\omega\Omega_e} = -i\frac{\omega_{pi}^2}{\omega\Omega_i}, \tag{6}$$

$$\epsilon^e_{yy} = 2\frac{\omega_{pe}^2}{\omega^2} z_e^2 \zeta_e Z(\zeta_e). \tag{7}$$

In Eqs. (6) and (7) plasma frequencies are denoted by ω_p and cyclotron frequencies by Ω. The second equality in Eq. (6) is approximately valid if the concentration of fusion ions is very low,[10] which is invariably the case for present experiments. In Eq. (7), $\zeta_e = \omega/k_z v_e$ and Z is the plasma dispersion function. It is useful to retain ϵ^e_{yy} in the calculation, since it describes the effects of transit time damping,[22] which is one of the dissipation mechanisms for the fast Alfvén wave. The appropriate expressions for the bulk ion dielectric tensor elements are the following:[23]

$$\epsilon^i_{xx} = \frac{\omega_{pi}^2}{\omega^2} \sum_{s=-\infty}^{\infty} \frac{s^2 e^{-z_i^2} I_s}{z_i^2} \zeta_0 Z(\zeta_s), \tag{8}$$

$$\epsilon^i_{xy} = i\frac{\omega_{pi}^2}{\omega^2} \sum_{s=-\infty}^{\infty} s e^{-z_i^2} \left(I_s' - I_s\right) \zeta_0 Z(\zeta_s), \tag{9}$$

$$\epsilon^i_{yy} = \frac{\omega_{pi}^2}{\omega^2} \sum_{s=-\infty}^{\infty} \left[\frac{s^2 e^{-z_i^2} I_s}{z_i^2} + 2z_i^2 e^{-z_i^2}\left(I_s - I_s'\right)\right] \zeta_0 Z(\zeta_\ell). \tag{10}$$

The corresponding expressions for the fusion ions can be obtained by substituting Eq. (1) into the general expressions for the dielectric tensor elements given, for example, in Ref. 23:

$$\epsilon^\alpha_{xx} = \frac{\omega_{p\alpha}^2}{\omega^2} \sum_{\ell=-\infty}^{\infty} \frac{\ell^2}{z_\alpha^2} \left[\left[-1 + (\eta_0 - \eta_\ell) Z(\eta_\ell)\right] z_\alpha \frac{dJ_\ell^2}{dz_\alpha} + \frac{2u^2}{v_r^2}\left[1 + \eta_\ell Z(\eta_\ell)\right] J_\ell^2\right], \tag{11}$$

$$\epsilon^{\alpha}_{xy} = i\frac{\omega^2_{p\alpha}}{\omega^2}\sum_{\ell=\infty}^{\infty}\frac{\ell}{z_\alpha}\left[[-1+(\eta_0-\eta_\ell)Z(\eta_\ell)]\frac{d}{dz_\alpha}(z_\alpha J_\ell J'_\ell)+\frac{2u^2}{v_r^2}[1+\eta_\ell Z(\eta_\ell)]\,J_\ell J'_\ell\right], \quad (12)$$

$$\epsilon^{\alpha}_{yy} = \frac{\omega^2_{p\alpha}}{\omega^2}\sum_{\ell=-\infty}^{\infty}\left[[-1+(\eta_0-\eta_\ell)Z(\eta_\ell)]\frac{1}{z_\alpha}\frac{d}{dz_\alpha}\left(z_\alpha^2\,(J'_\ell)^2\right)+\frac{2u^2}{v_r^2}[1+\eta_\ell Z(\eta_\ell)]\,(J'_\ell)^2\right]. \quad (13)$$

Here, I_s is the modified Bessel function of the first kind of order s, and J_ℓ is the Bessel function of the first kind of order ℓ. The argument of I_s is $z_i^2 = k_x^2 v_i^2/2\Omega_i^2$, where v_i is the bulk ion thermal speed, and the argument of J_ℓ is $z_\alpha = k_x u/\Omega_\alpha$. The argument of Z is

$$\zeta_s = \frac{\omega - s\Omega_i}{k_z v_i}, \quad (14)$$

in Eqs. (8) – (10), and

$$\eta_\ell = \frac{\omega - k_z v_d - \ell\Omega_\alpha}{k_z v_r}, \quad (14)$$

in Eqs. (11) – (13). Finally, θ is the propagation angle of the wave, i.e. $\cos\theta = k_z/k$. We have implicitly assumed that $\theta \leq 90°$: when $\theta > 90°$, $Z(\zeta_s)$ and $Z(\eta_\ell)$ must be replaced with $-Z(-\zeta_s)$ and $-Z(-\eta_\ell)$ respectively in Eqs. (8) – (13).[22]

It should be noted that the expressions for ϵ^i_{ij} include a description of θ–dependent wave–particle cyclotron damping by the bulk ions. In the case of $k_z = 0$, considered in Refs. 9 and 10, cyclotron damping is absent, and its role in reducing the degree of possible instability is taken over in this limit by the positive–energy loading associated with resonant cyclotron harmonic waves supported by the bulk ions. Our calculations of the maximally unstable propagation angle reflect the fact that the stabilizing effect of positive–energy loading, represented by the modified Bessel function terms in Eqs. (8) – (10), is also θ–dependent.

IV. PERTURBATIVE ANALYSIS

Following the approach used in Ref. 10, we consider the resonant excitation of a fast Alfvén wave at frequencies lying close to the energetic ion cyclotron frequency and its harmonics. Since the concentration of fusion ions is very low, the fast Alfvén wave is supported by the bulk ions and electrons. Under these conditions, we can carry out a perturbation analysis. In order to obtain the appropriate dispersion relation it is helpful to separate the terms in Eq. (2) which depend only on ϵ^i_{ij} and ϵ^e_{ij} from those which depend on ϵ^α_{ij}. Placing the latter on the right hand side, and writing $n_\parallel = k_z c/\omega$, $n_\perp = k_x c/\omega$ we obtain

$$(\epsilon^i_{xx} - n_\parallel^2)n_\perp^2 - (\epsilon^i_{yy} - n_\parallel^2)(\epsilon^i_{xx} - n_\parallel^2) - (\epsilon^e_{xy} + \epsilon^i_{xy})^2 - \epsilon^e_{yy}(\epsilon^i_{xx} - n_\parallel^2)$$

$$= -\epsilon^\alpha_{xx}n_\perp^2 + (\epsilon^i_{yy} - n_\parallel^2)\epsilon^\alpha_{xx} + (\epsilon^i_{xx} - n_\parallel^2)\epsilon^\alpha_{yy} + 2(\epsilon^e_{xy} + \epsilon^i_{xy})\epsilon^\alpha_{xy} + \epsilon^\alpha_{xx}(\epsilon^\alpha_{yy} + \epsilon^e_{yy}) + {\epsilon^\alpha_{xy}}^2. \quad (16)$$

As in Ref. 10, we assume that ϵ^i_{xx}, ϵ^i_{xy} and ϵ^i_{yy} can each be approximated by two terms: a cold part, corresponding to $s = \pm 1$; and a resonant part, corresponding to s such that $s\Omega_i$ is the bulk ion cyclotron harmonic lying closest to ω. We assume for the time being that $s \neq 1$. If $z_i^2 \ll 1$, we can then write

$$\epsilon^i_{xx} = -\frac{\omega_{pi}^2}{\omega^2 - \Omega_i^2} + \frac{\omega_{pi}^2}{\omega^2}\frac{s^2}{2^s s!} z_i^{2(s-1)}\zeta_0 Z(\zeta_s), \quad (17)$$

$$\epsilon^i_{xy} = -i\frac{\omega_{pi}^2}{\omega^2 - \Omega_i^2}\frac{\Omega_i}{\omega} + i\frac{\omega_{pi}^2}{\omega^2}\frac{s^2}{2^s s!} z_i^{2(s-1)}\zeta_0 Z(\zeta_s), \quad (18)$$

$$\epsilon^i_{yy} = -\frac{\omega_{pi}^2}{\omega^2 - \Omega_i^2} + \frac{\omega_{pi}^2}{\omega^2}\frac{s^2}{2^s s!} z_i^{2(s-1)}\zeta_0 Z(\zeta_s). \quad (19)$$

In order to proceed analytically it is necessary to make two further assumptions. First, we assume that only those terms corresponding to ℓ such that $\ell\Omega_\alpha = s\Omega_i$ contribute significantly to the summations in Eqs. (11) – (13). Second, we assume that the ratio of fusion ion number density to bulk ion number density, denoted here by ξ, is sufficiently small that the last two terms on the right hand side of Eq. (16), which are quadratic in $\omega_{p\alpha}^2$, can be neglected. Substituting Eqs. (6), (11) – (13) and (17) – (19) in Eq. (16), and neglecting terms proportional to $\omega_{p\alpha}^4$ and $z_i^{2(s-1)}\omega_{p\alpha}^2$, we obtain the dispersion relation

$$\omega^2 - a^2 k_x^2 c_A^2 =$$

$$-\Omega_i^2 \frac{(\omega-\Omega_i)\left((\omega+\Omega_i)\left(\frac{1}{2}N_\perp^2+N_\parallel^2\right)-\Omega_i\right)}{\left(\Omega_i+(\omega-\Omega_i)N_\parallel^2\right)\left(\Omega_i-(\omega+\Omega_i)N_\parallel^2\right)} \frac{s^2}{2^{s-1}s!} z_i^{2(s-1)} \zeta_0 Z(\zeta_s) - 2\Omega_i^2 \frac{\omega_{pe}^2}{\omega_{pi}^2} a^2 z_e^2 \zeta_e^2 Z(\zeta_e)$$

$$+ \frac{\omega_{p\alpha}^2}{\omega_{pi}^2} \frac{\Omega_i^4}{\left(\Omega_i+(\omega-\Omega_i)N_\parallel^2\right)\left(\Omega_i-(\omega+\Omega_i)N_\parallel^2\right)}$$

$$\times \left[\left(-1+(\eta_0-\eta_\ell)Z(\eta_\ell)\right)M_\ell - \frac{2u^2}{v_r^2}\left(1+\eta_\ell Z(\eta_\ell)\right)N_\ell\right], \tag{20}$$

where c_A is the Alfvén speed, $N_\parallel = k_z c_A/\omega$, $N_\perp = k_x c_A/\omega$, and the quantities a^2, M_ℓ and N_ℓ are defined as follows:

$$a^2 = \frac{\Omega_i^2 + (\omega^2 - \Omega_i^2)N_\parallel^2}{\left(\Omega_i+(\omega-\Omega_i)N_\parallel^2\right)\left(\Omega_i-(\omega+\Omega_i)N_\parallel^2\right)}, \tag{21}$$

$$M_\ell = 2\ell\frac{\omega}{\Omega_i}\left[J_\ell'^2 + \frac{1}{z_\alpha^2}(\ell^2 - z_\alpha^2)J_\ell^2\right] - 2\frac{\omega^2-\Omega_i^2}{\Omega_i^2}\frac{J_\ell J_\ell'}{z_\alpha}\left[\ell^2 N_\perp^2 + (2\ell^2 - z_\alpha^2)N_\parallel^2\right] + \frac{2J_\ell J_\ell'}{z_\alpha}(z_\alpha^2 - 2\ell^2), \tag{22}$$

$$N_\ell = -2\ell\frac{\omega}{\Omega_i}\frac{J_\ell J_\ell'}{z_\alpha} + \frac{\omega^2-\Omega_i^2}{\Omega_i^2}\left[N_\parallel^2\left(\frac{\ell^2 J_\ell^2}{z_\alpha^2} + J_\ell'^2\right) + N_\perp^2\frac{\ell^2 J_\ell^2}{z_\alpha^2}\right] + \frac{\ell^2 J_\ell^2}{z_\alpha^2} + J_\ell'^2. \tag{23}$$

The second derivative of J_ℓ, which appears in ϵ_{xy}^α and ϵ_{yy}^α, has been eliminated from the expression for M_ℓ using Bessel's equation.

The terms on the right hand side of Eq. (20) arise from the finite temperature of the bulk ions and electrons, and from the presence of fusion products. Setting these terms equal to zero yields the dispersion relation for obliquely propagating electromagnetic waves in a cold plasma:

$$\omega^2 = a^2 k_x^2 c_A^2. \tag{24}$$

Equation (24) is a quadratic equation for ω^2 with solution

$$\omega^2 = \frac{1}{2}c_A^2\left[k^2 + k_z^2 + k^2 k_z^2 \frac{c_A^2}{\Omega_i^2} \pm \sqrt{\left(k^2 + k_z^2 + k^2 k_z^2\frac{c_A^2}{\Omega_i^2}\right)^2 - 4k^2 k_z^2}\right]. \tag{25}$$

The plus sign in Eq. (25) corresponds to the fast (compressional) Alfvén wave, while the minus sign corresponds to the shear Alfvén wave. This can be easily verified by considering the MHD limit, $\omega \ll \Omega_i$.

We now seek perturbative solutions of the dispersion relation Eq. (20) by writing

$$\omega = \omega_0 + \delta\omega, \tag{26}$$

where ω_0 is the real frequency given by the plus sign in Eq. (25), $\delta\omega$ is complex, and we assume that $|\delta\omega| \ll \omega_0$. This is valid if ξ is sufficiently small. Under these circumstances we can replace ω with ω_0 on the right hand side of Eq. (20). We assume that, in Eq. (1), $v_d \gg v_i$ and $v_r \gg v_i$, which means that any waves with $k_z \neq 0$ are significantly Doppler–shifted between the guiding centre rest frame of the fusion ions and that of the bulk ions. Thus, when the fusion ions are in cyclotron resonance with the fast wave, the bulk ions will be out of resonance, and bulk ion cyclotron damping can be neglected. In this case $|\zeta_s| \gg 1$, so that

$$\zeta_0 Z(\zeta_s) \simeq -\frac{\omega_0}{\omega_0 - s\Omega_i}, \tag{27}$$

whereas $|\eta_\ell|$ can be of order unity or less, and so it is necessary to take into account the imaginary part of $Z(\eta_\ell)$. Since, in our perturbation analysis, η_ℓ is real, it follows that

$$\mathrm{Im}\,(Z(\eta_\ell)) = \sqrt{\pi}e^{-\eta_\ell^2}. \tag{28}$$

Finally, we assume for the time being that transit time damping (which arises from the electron term on the right hand side of Eq. (20)) can be neglected. Under these circumstances, it follows immediately that the perturbative solution for the imaginary part of $\delta\omega$ is the following:

$$\gamma \equiv \mathrm{Im}(\delta\omega) \simeq$$

$$\frac{\omega_{p\alpha}^2}{\omega_{pi}^2}\frac{\Omega_i^4}{\left(\Omega_i + (\omega_0 - \Omega_i)N_\parallel^2\right)\left(\Omega_i - (\omega_0 + \Omega_i)N_\parallel^2\right)}\left[\frac{\ell\Omega_\alpha}{k_z v_r}M_\ell - \frac{2u^2}{v_r^2}\eta_\ell N_\ell\right]\frac{\sqrt{\pi}}{2\omega_0}e^{-\eta_\ell^2}. \tag{29}$$

For completeness, we also give the solution for the real part of $\delta\omega$, although the relevant parameters are such that it is often sufficiently accurate to set $\mathrm{Re}(\omega) = \omega_0$:

$$\mathrm{Re}(\delta\omega) \simeq \frac{(\omega_0 - \Omega_i)\left((\omega_0 + \Omega_i)\left(N_\perp^2/2 + N_\parallel^2\right) - \Omega_i\right)}{\left(\Omega_i + (\omega - \Omega_i)N_\parallel^2\right)\left(\Omega_i - (\omega + \Omega_i)N_\parallel^2\right)} \frac{1}{\omega_0 - s\Omega_i} \frac{s^2}{2^s s!} z_i^{2(s-1)}. \tag{30}$$

In deriving this expression we have assumed that ξ is sufficiently small that the dominant real contribution to the right hand side of Eq. (20) comes from the bulk ion term. In Eqs. (29) and (30) η_ℓ, M_ℓ, N_ℓ, $N_\parallel$ and $N_\perp$ are evaluated for $\omega = \omega_0$. In the special case $s = 1$, the imaginary part of $\delta\omega$ is still given by Eq. (29), while $\mathrm{Re}(\delta\omega) \simeq 0$. Positive (negative) values of $\mathrm{Im}(\delta\omega)$ indicate wave growth (damping). In the case of fusion alpha particles in a deuterium plasma, $\Omega_\alpha = \Omega_i$ and so $\ell = s$.

Equations (25), (29) and (30) give ω as a function of k, θ, and the distribution function parameters. The exponential factor in Eq. (29) indicates that a strong wave–particle interaction will only occur if $|\eta_\ell|$ is of order unity or less. It is clear that both growth and damping are possible, depending on the sign of the quantity in square brackets in Eq. (29). N_ℓ is generally positive, and so the term containing this quantity is only destabilizing if $\eta_\ell < 0$, in which case the wave frequency, Doppler–shifted into a frame moving with speed v_d along the magnetic field direction, lies below $\ell\Omega_\alpha$. On the other hand, M_ℓ can be positive or negative, depending on z_α and ℓ. We note that the growth or damping rate has a simple linear dependence on ξ: in the absence of electron Landau damping and transit time damping, instability can occur for all values of ξ. In the case of $k_z = 0$, the growth rate is proportional to $\xi^{1/2}$ if the plasma is cold, but positive–energy loading in a warm plasma leads to the suppression of instability when the concentration of fusion products is sufficiently low.[9,10]

The perturbative analysis described above can also be used to derive the transit time damping rate, γ_e. Again setting $\omega = \omega_0$ on the right hand side of Eq. (20), and using Eq.

(28), it is straightforward to show that

$$\gamma_e = \frac{\sqrt{\pi}}{2}\omega_0 a^2 \frac{m_e}{m_i}\frac{n_e}{n_i}\frac{v_e^2}{c_A^2}\zeta_e e^{-\zeta_e^2}, \tag{31}$$

where particle masses are denoted by m and densities by n. An important point to note is that γ_e is independent of ξ, and so transit time damping will suppress the magnetoacoustic cyclotron instability if the concentration of fusion ions is sufficiently low. When the z component of the wave electric field $\mathbf{E}$ is finite, one must also take into account electron Landau damping and an effect arising from the phase difference between E_y and E_z.[22] The overall effect of electron dissipation on the fast wave can be quantified by computing the power absorbed by the electrons, and dividing this by the wave energy density. When ω lies in the ion cyclotron range and $\omega_{pi}^2 \gg c^2k_z^2$, the result is that the total electron damping rate is one half of the transit time damping rate.[22] Equation (31) thus gives the correct order of magnitude of the electron dissipation, and can be used to estimate the threshold value of ξ required for instability. We have assumed that $E_z = 0$, which means that our analysis does not incorporate Landau damping. Since transit time damping and electron Landau damping are of comparable magnitude and are non–negligible in the same parameter régime, namely $|\zeta_e| \lesssim 1$, it is inconsistent to describe the effects of the former while neglecting the latter. For this reason, all the numerical results presented in the next section were obtained with ϵ_{yy}^e set equal to zero.

V. APPLICATION TO ICE IN JET

The full dispersion relation Eq. (16) can readily be solved numerically for $w \equiv \omega/\Omega_\alpha$ as a function of z_α and θ. If ω and $\mathbf{k}$ are normalized in this way, and the masses and charges of the ion species are specified, solutions of Eq. (16) depend on six dimensionless parameters, which may conveniently be chosen to be the following: the local concentration of fusion ions, ξ; the local bulk ion plasma beta, $\beta_i \equiv (1-\xi)v_i^2/c_A^2$; the ratio of the fusion ion ring speed to the Alfvén speed, u/c_A; the ratio of the fusion ion parallel drift speed to the ring speed, v_d/u; the ratio of the fusion ion parallel velocity spread to the ring speed, v_r/u; and the electron–ion temperature ratio, T_e/T_i. This last parameter appears only in the transit time damping term, which we neglect for the reason stated at the end of the last section. For the case of the preliminary tritium experiments on JET, we can make realistic estimates of all the remaining parameters using the results presented in Ref. 7. We assume a magnetic field of 2.07 T, a bulk ion density of 1.7×10^{19} m^{-3} (cf. Fig. 6 of Ref. 7), and a bulk ion temperature of 1 keV. Given that the energy of alpha-particles reaching the edge plasma is close to the birth energy of 3.5 MeV (cf. Fig. 15 of Ref. 7), it follows that $\beta_i \simeq 1.6 \times 10^{-3}$ and $u \simeq 1.67 c_A$. From Fig. 16 of Ref. 7 we infer, furthermore, that $v_d \simeq 0.25u$ and $v_r \simeq 0.05u$, while Fig. 6 of Ref. 7 indicates that $\xi < 10^{-4}$ in the edge plasma. It turns out that the transit time damping rate given by Eq. (31) is generally negligible for propagation angles lying in the range $60° < \theta < 120°$, whenever $\xi > 10^{-6}$. For this reason, numerical results were obtained for θ lying within $\pm 30°$ of the perpendicular, and for ξ lying in the range 10^{-6}–10^{-4}.

We begin by testing the accuracy of Eqs. (29) and (30). In Fig. 1, γ is plotted as a function of $\omega' = \omega - k_z v_d$ for $\theta = 85°$. Numerical results are indicated by solid curves, and analytical results by dashed curves. The distribution function parameters are those given above. Two values of ξ are used: 10^{-4} (upper frame) and 10^{-6} (lower frame). In the latter case there is excellent agreement between the analytical and exact solutions, except in the vicinity of $\omega = \Omega_\alpha = \Omega_i$. At this frequency there is significant cyclotron damping due to the bulk ions. This effect was neglected in Eq. (29), but would have been straightforward to incorporate by allowing $Z(\zeta_s)$ in Eq. (20) to be complex rather than real. The point we wish to emphasize here is that the damping which occurs at $\omega' \simeq \Omega_\alpha$ in Fig. 1 can be attributed solely to the *fusion* ions, and has nothing to do with the *bulk* ions. The quantity M_ℓ is negative, and so waves with $\omega' > \Omega_\alpha$ are damped, as expected. The agreement between the analytical and numerical solutions becomes less good when the concentration of fusion ions is increased from 10^{-6} to 10^{-4}. The corresponding results for $\omega' \sim 4\Omega_\alpha$ are shown in Fig. 2. M_ℓ is now positive, and so instability can occur at $\omega' > 4\Omega_\alpha$. As in Fig. 1, the analytical solution becomes less accurate as ξ is increased.

We now proceed to compute the growth rates of all cyclotron harmonics up to $\ell = 10$ at various propagation angles ranging from 80° to 100°. The results are shown in Fig. 3, plotted as a function of ω rather than ω'. We are thus able to highlight the Doppler effect introduced by $v_d \neq 0$. The fusion ion concentration is 10^{-4}, and the other distribution function parameters are identical to those used to generate Figs. 1 and 2. In the case of perpendicular propagation the line profiles are extremely narrow, and not all cyclotron harmonics are unstable at a given locus (cf. upper frame of Fig. 18 in Ref. 7). The narrow bandwidths arise from the fact that $f_\alpha \propto \delta(v_\perp - u)$ (the distribution of parallel speeds is irrelevant when $k_z = 0$). Cyclotron resonance of the perpendicular–propagating fast Alfvén wave with the fusion ions can imply stability or instability,[9,10] depending on the value of z_α. The stability of the second cyclotron harmonic can be attributed to the positive–energy loading associated with bulk ion–supported ion Bernstein waves (see Fig. 2 in Ref. 17). In the oblique case, we find that every cyclotron harmonic is linearly unstable at all propagation angles, except $\theta \simeq 90°$. Computing the maximum growth rate corresponding to particular cyclotron harmonics, we find in most cases that there are two local maxima in the function $\gamma(k, \theta)$, one on either side of $\theta = 90°$. Because of Doppler shifts, these local maxima correspond to frequencies lying above and below $\ell\Omega_\alpha$ (compare, for example, Fig. 3(b) with Fig. 3(d)). The difference between the two frequencies is given by

$$\Delta\omega = \Delta k_z v_d = \Delta(z_\alpha \cot\theta)\frac{v_d}{u}\Omega_\alpha. \tag{32}$$

The maximally unstable propagation angles range from 67° and 102° in the case of $\ell = 1$ to 84° and 95° in the case of $\ell = 10$. The corresponding values of $\Delta\omega$ are $0.26\Omega_\alpha$ and $0.64\Omega_\alpha$ respectively. These figures are consistent with the magnitude of line splitting observed in ICE spectra from both pure deuterium and mixed deuterium–tritium discharges.[7] Line splitting in our model arises from the fact that $v_d \neq 0$, and so the fine structure of ICE spectra may arise from the drifting of fusion ions along the magnetic field. We note, however, that line splitting may also occur as a result of the diamagnetic drift associated with a pressure gradient.

The most important new result to emerge from the above analysis is that all harmonics of the fusion ion cyclotron frequency, including the fundamental, can be simultaneously excited. This is only true for obliquely propagating waves: when $k_z = 0$, only a few cyclotron harmonics are simultaneously unstable, and the effects of positive–energy loading mean that instability cannot occur unless ξ lies above an ℓ–dependent threshold.[9,17] In the $k_z \neq 0$ case, Eq. (29) suggests that wave excitation is possible for arbitrarily low values of ξ. In practice, because of electron Landau damping and transit time damping, there will be a threshold concentration for instability, but Eq. (31) indicates that this threshold will be extremely low whenever $|\zeta_e| < 1$.

This last result raises the possibility that small numbers of secondary alpha-particles, born from the reaction of deuterons with primary tritons or helium–3 nuclei, could excite the magnetoacoustic cyclotron instability, thus giving rise to wave emission at frequencies lying close to harmonics of the deuteron cyclotron frequency. In the case of pure deuterium ohmic discharges, the only primary fusion products which appear to be capable of driving the magnetoacoustic cyclotron instability are protons.[10] Fusion protons cannot, however, account for the observed excitation of odd deuteron harmonics,[2] since the proton cyclotron frequency is twice that of the deuteron. Our analysis shows that odd deuteron harmonics can be driven unstable in a pure deuterium discharge by a very low concentration of secondary alpha-particles. Since γ varies linearly with ξ, it is likely that the instability is very weak, but it may nevertheless be possible to account for the presence of odd deuteron harmonics using this mechanism. It is worth noting in this context that odd deuteron harmonics are often observed to be less intense than even ones, both in pure deuterium ohmic discharges,[2,7] and in the JET tritium experiments.[7] In the latter case, the presence of primary protons, in addition to primary alpha particles, could account for the higher intensity of the even harmonics. However, given the present lack of knowledge of the nonlinear saturation mechanism, it is difficult to draw firm conclusions.

VI. PROPAGATION AND ABSORPTION

Figs. 1 and 2 exemplify two qualitatively different situations: in Fig. 1, instability only occurs on the low frequency side of cyclotron resonance, and is accompanied by much stronger damping on the high frequency side; in Fig. 2, wave growth occurs on both sides of cyclotron resonance, and damping is relatively weak. In order to reach the plasma edge, a wave generated inside a tokamak must traverse a diminishing magnetic field, and so it is likely that, before being detected, a wave which initially satisfies $\omega' < \ell\Omega_\alpha$ will encounter a region in which the opposite inequality applies. If M_ℓ is sufficiently large and positive, as in Fig. 2, the wave will continue to grow as it propagates. If, however, M_ℓ is negative, as in Fig. 1, a wave which is unstable in one region of the plasma may be strongly damped before it reaches the antenna. Thus, the wave is more likely to be detectable if $M_\ell > 0$. It is therefore important to establish the parameter régime in which this inequality is satisfied. Fig. 4 shows M_1 as a function of z_α for two different propagation angles and, as before, $u = 1.67c_A$. M_1 has been evaluated using $\omega = \omega_0$. The bold lines indicate the range of values of z_α such that the obliquely propagating fast Alfvén wave is in cyclotron resonance with a significant number of fusion ions. Specifically, we have set

$$\omega = ak_x c_A = \Omega_\alpha + k_z v_\parallel, \tag{33}$$

where

$$v_d - 2v_r < v_\parallel < v_d + 2v_r, \tag{34}$$

so that $\exp(-\eta_\ell^2) > 10^{-2}$. As before, $v_d = 0.25u$ and $v_r = 0.05u$. The important point is that $M_1 < 0$ for all resonant values of z_α, and in fact this result holds for all propagation angles lying within $\pm 20°$ of the perpendicular direction. When $\theta \simeq 125°$ we find that $M_1 > 0$ for resonant values of z_α, but in this case M_1 is so small that the line profile is dominated by the N_1 term in Eq. (29). At such large values of $|90° - \theta|$, Eq. (31) indicates that the instability will, in any case, be suppressed by transit time damping. It thus appears that fundamental cyclotron waves generated by fusion ions in the edge plasma may undergo attenuation before reaching the detector, although this will depend on how steeply the fusion ion density falls off with radius in the edge plasma. Similar remarks apply to the case of second harmonic cyclotron waves.

Fig. 5 shows the corresponding results for $\ell = 4$. In this case the value of M_ℓ in the resonant region of z_α space is rather sensitive to θ: it is strongly positive when $\theta = 85°$, and approximately zero when $\theta = 80°$. We find generally that $M_\ell < 0$ at resonance for all $\ell \geq 3$, except when θ lies within a few degrees of the perpendicular direction.

VII. CONCLUSIONS AND DISCUSSION

In this paper we have studied the excitation of obliquely propagating fast Alfvén waves by the magnetoacoustic cyclotron instability, driven by a drifting ring–like distribution of fusion ions. Restricting our analysis to cases in which electron Landau damping can be neglected, we have obtained a perturbative solution of the appropriate dispersion relation, which, in the relevant parameter régime, reproduces many of the essential features of the exact numerical solutions presented in Sec. V. By extending the previously existing theory of the magnetoacoustic cyclotron instability from perpendicular to oblique propagation, we have shown that linear instability can occur at the fusion ion cyclotron frequency and all its harmonics. Using a model velocity–space distribution for the fusion ions appropriate to the ion cyclotron emitting region in JET tritium experiments,[7] we have shown that the finite parallel wave number effectively decouples the magnetoacoustic cyclotron instability from bulk ion cyclotron damping. The parallel drift of the fusion ions provides a simple (although not necessarily unique) possible explanation of the observed splitting of harmonic emission lines. Finally, the predicted persistance of the instability when the concentration of fusion ions is extremely low suggests that secondary alpha-particles may be capable of exciting the hitherto unexplained wave emission at odd deuteron harmonics in pure deuterium ohmic discharges.

Our analysis has been restricted to linear Vlasov theory in the locally uniform approximation: we have not addressed at all the question of wave saturation, and we have only touched briefly on the problem of wave propagation from the source region to the detector. In Sec. VI we argued that a cyclotron harmonic wave may undergo significant attenuation if the function M_ℓ defined in Eq. (22) is negative. At the maximally unstable propagation angle, $M_\ell < 0$ for $\ell = 1$ and $\ell = 2$. In order to ascertain whether or not our model can account for the appearance of those harmonics in ICE spectra, it would be necessary to specify the magnetic geometry and spatial distribution of alpha particles in the edge plasma, and to carry out a full wave calculation. When the concentration of fusion ions is very low, electron dissipation may be significant in the case of the lowest cyclotron harmonics: when $\xi = 10^{-6}$, the transit time damping rate of the fundamental $\ell = 1$ mode given by Eq. (31) is comparable to the magnetoacoustic cyclotron growth rate at the smaller of the two maximally unstable propagation angles. In such cases it might be desirable to solve the full dispersion relation, allowing the z component of the electric field to be finite.

ACKNOWLEDGMENTS

This work was funded jointly by the UK Department of Trade and Industry and Euratom. We are grateful to T. J. Martin for providing us with a general purpose zero finding code.

REFERENCES

[1] G. A. Cottrell, P. P. Lallia, G. Sadler, and P. van Belle, in *Proceedings of the 13th European Conference on Controlled Fusion and Plasma Heating*, Schliersee, Germany, 1986, edited by G. Briffod and M. Kaufmann (European Physical Society, Petit-Lancy, Switzerland, 1986), Part II, Vol. 10C, p. 37.

[2] G. A. Cottrell and R. O. Dendy, Phys. Rev. Lett. **60**, 33 (1988).

[3] P. Schild, G. A. Cottrell and R. O. Dendy, Nucl. Fusion **29**, 834 (1989).

[4] G. J. Greene and the TFTR Team, in *Proceedings of the 17th European Conference on Controlled Fusion and Plasma Heating*, Amsterdam, Netherlands, 1990, edited by G. Briffod, Adri Nijsen-Vis, and F. C. Schüller (European Physical Society, Petit-Lancy, Switzerland, 1990), Part IV, Vol. 14B, p. 1540.

[5] G. A. Cottrell, V. P. Bhatnagar, O. da Costa, R. O. Dendy, A. Edwards, J. Jacquinot, F. Nave, M. Schmid, A. Sibley, P. Smeulders, and D. F. H. Start, in *Proceedings of the 19th European Conference on Controlled Fusion and Plasma Heating*, Innsbruck, Austria, 1992, edited by W. Freysinger, K. Lackner, R. Schrittwieser, and W. Lindinger (European Physical Society, Petit-Lancy, Switzerland, 1990), Part I, Vol. 16C, p. 327.

[6] The JET Team, Nucl. Fusion **32**, 187 (1992).

[7] G. A. Cottrell, V. P. Bhatnagar, O. da Costa, R. O. Dendy, J. Jacquinot, K. G. McClements, D. C. McCune, M. F. F. Nave, P. Smeulders, and D. F. H. Start, Nucl. Fusion, in press (1993).

[8] R. O. Dendy, in *Theory of Fusion Plasmas.* edited by E. Sindoni and J. Vaclavik (Editrice Compositori, Bologna, 1992), p. 41.

[9] V. S. Belikov and Ya. I. Kolesnichenko, Sov. Phys. Tech. Phys. **20**, 1146 (1975).

[10] R. O. Dendy, C. N. Lashmore–Davies, and K. F. Kam, Phys. Fluids B **4**, 3996 (1992).

[11] R. O. Dendy, C. N. Lashmore–Davies, and K. F. Kam, Phys. Fluids B **5**, 1937 (1993).

[12] L. V. Korablev, Sov. Phys. JETP **26**, 922 (1968).

[13] T. D. Kaladze, D. G. Lominadze, and K. N. Stepanov, Sov. Phys. Tech. Phys. **19**, 175 (1974).

[14] T. D. Kaladze and A. B. Mikhailovskii, Sov. J. Plasma Phys. **1**, 128 (1976).

[15] B. Coppi, S. Cowley, R. Kulsrud, P. Detragiache, and F. Pegoraro, Phys. Fluids **29**, 4060 (1986).

[16] M. Lisak, H. Hamnén, and D. Anderson, J. Plasma Phys. **45**, 229 (1991).

[17] K. G. McClements and R. O. Dendy, J. Geophys. Res. **98**, 11,689 (1993).

[18] R. O. Dendy and K. G. McClements, J. Geophys. Res. **98**, 15,531 (1993).

[19] D. J. Sigmar, in *Proceedings of the Varenna Course on Physics of Plasmas Close to Thermonuclear Conditions*, Varenna, 1979 (Commission of the European Communities, Brussels, 1980), Vol. I, p. 271.

[20] D. G. Lominadze and A. B. Mikhailovskii, Sov. J. Plasma Phys. **1**, 291 (1975).

[21] V. S. Belikov, Ya. I. Kolesnichenko, and A. D. Fursa, in *Plasma Physics and Controlled Nuclear Fusion Research 1978* (International Atomic Energy Agency, Vienna, 1979), Vol. I, p. 561.

[22] T. H. Stix, Nucl. Fusion **15**, 737 (1975).

[23] T. H. Stix, *Waves in Plasmas* (American Institute of Physics, New York, 1992).

Figure Captions

FIG. 1. Growth/damping rate as a function of $\omega' = \omega - k_z v_d$ for the case of energetic alpha particles in a deuterium plasma. Numerical results are indicated by solid curves, and analytical results by dashed curves. The distribution function parameters other than ξ are the following: $\beta_i = 1.6 \times 10^{-3}$, $u/c_A = 1.67$, $v_d/u = 0.25$, and $v_r/u = 0.05$. The wave propagation angle is 85°.

FIG 2. As Fig. 1 except that $\omega' \simeq 4\Omega_\alpha$.

FIG. 3. Growth rate as a function of ω for propagation angles ranging from 80° to 100°. The concentration of fusion ions is 10^{-4}, and the other distribution function parameters are identical to those used to generate Figs. 1 and 2.

FIG 4. M_1 as a function of z_α for two values of θ and $u = 1.67c_A$. The bold lines indicate the range of values of z_α such that the fast Alfvén wave resonance condition is satisfied, assuming $v_d = 0.25u$ and $v_r = 0.05u$.

FIG. 5. As Fig. 4 except that $\ell = 4$.

FIGURE 1

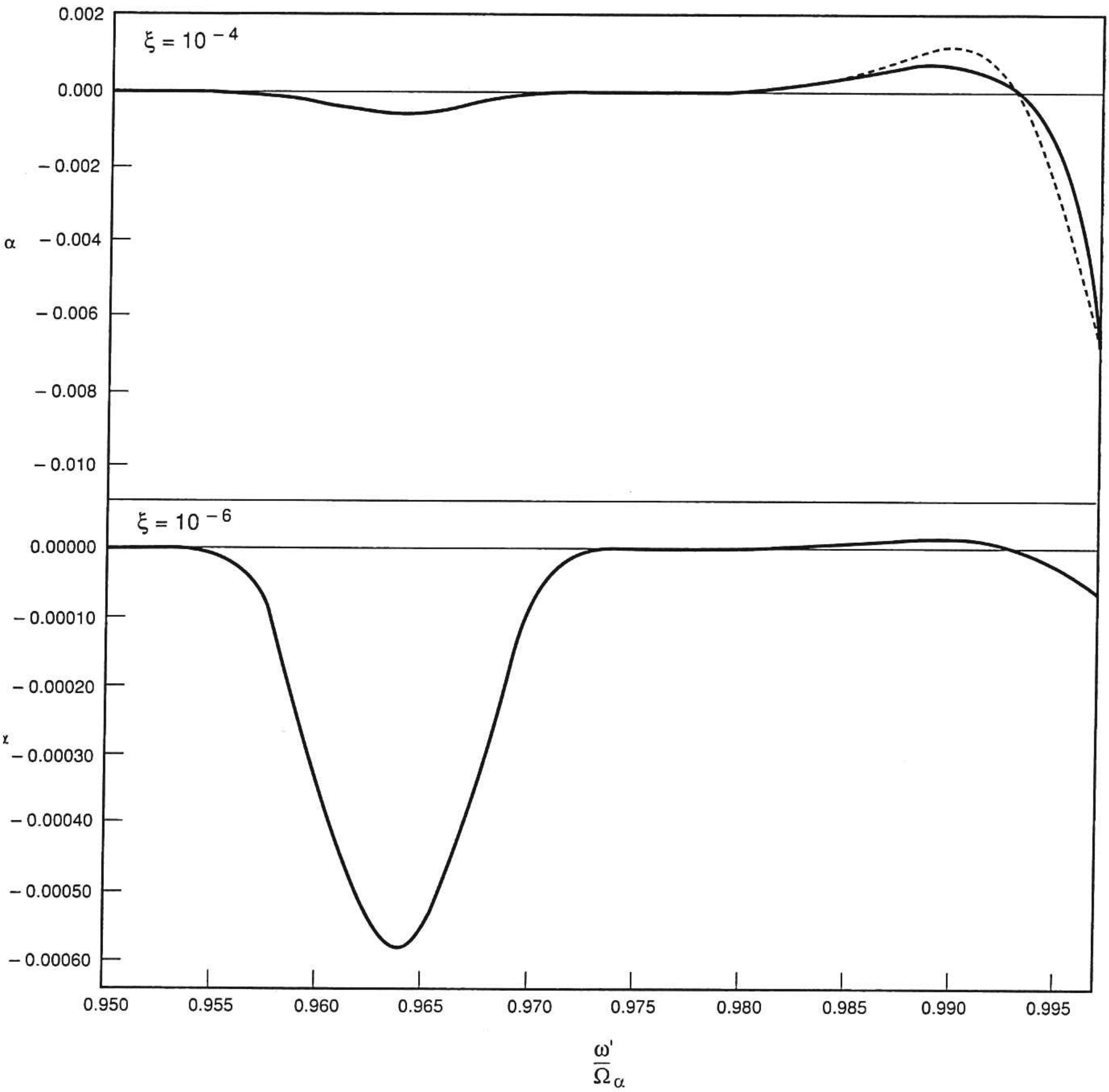

$\xi = 10^{-4}$
0.002
0.000
− 0.002
α
− 0.004
− 0.006
− 0.008
− 0.010
$\xi = 10^{-6}$
0.00000
− 0.00010
− 0.00020
χ
− 0.00030
− 0.00040
− 0.00050
− 0.00060
0.950
0.955
0.960
0.965
0.970
0.975
0.980
0.985
0.990
0.995
$\frac{\omega'}{\Omega_\alpha}$

FIGURE 2

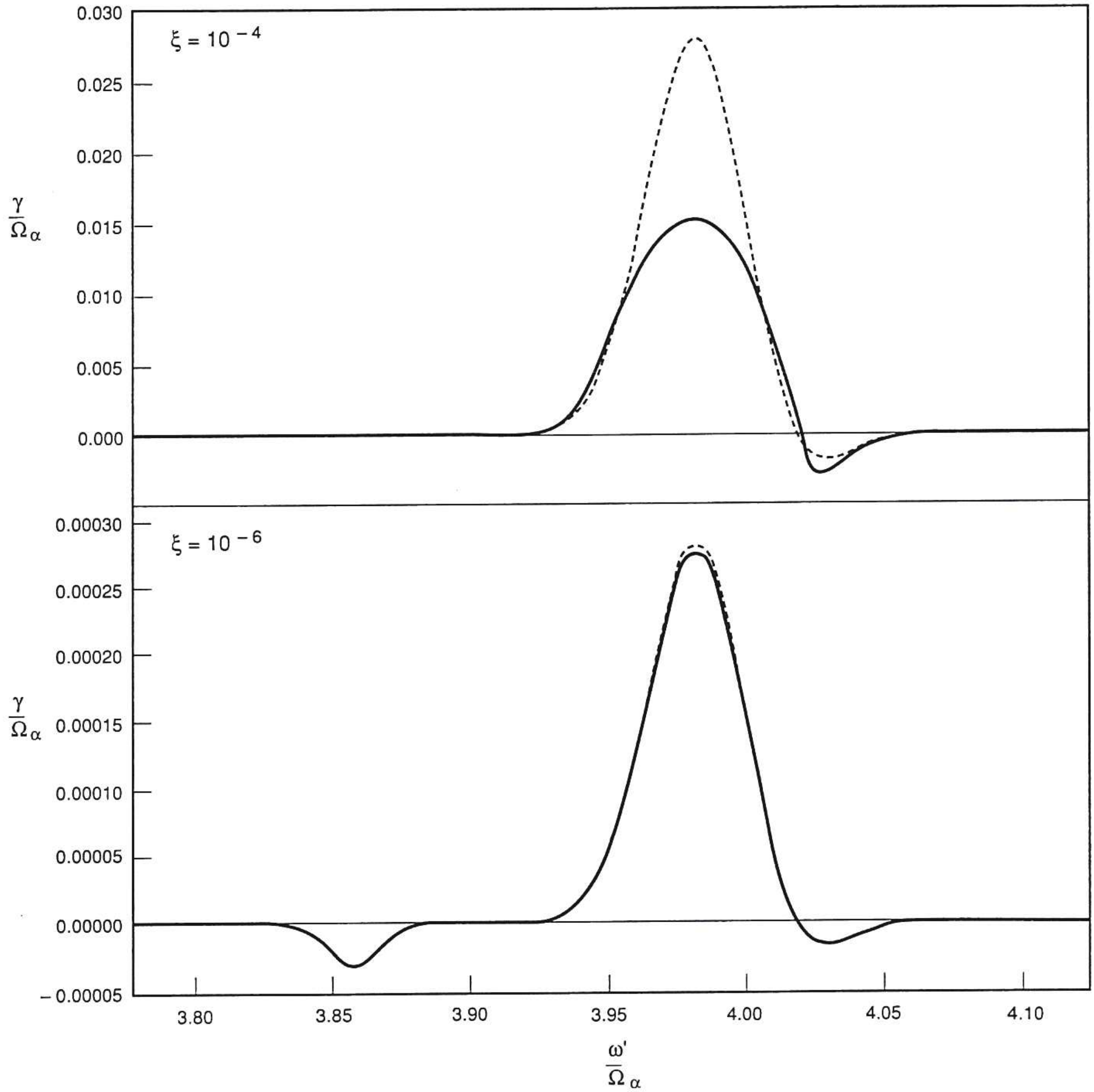

0.030
0.025
0.020
0.015
0.010
0.005
0.000
$\xi = 10^{-4}$
$\frac{\gamma}{\Omega_\alpha}$
0.00030
0.00025
0.00020
0.00015
0.00010
0.00005
0.00000
− 0.00005
$\xi = 10^{-6}$
$\frac{\gamma}{\Omega_\alpha}$
3.80
3.85
3.90
3.95
4.00
4.05
4.10
$\frac{\omega'}{\Omega_\alpha}$

FIGURE 3

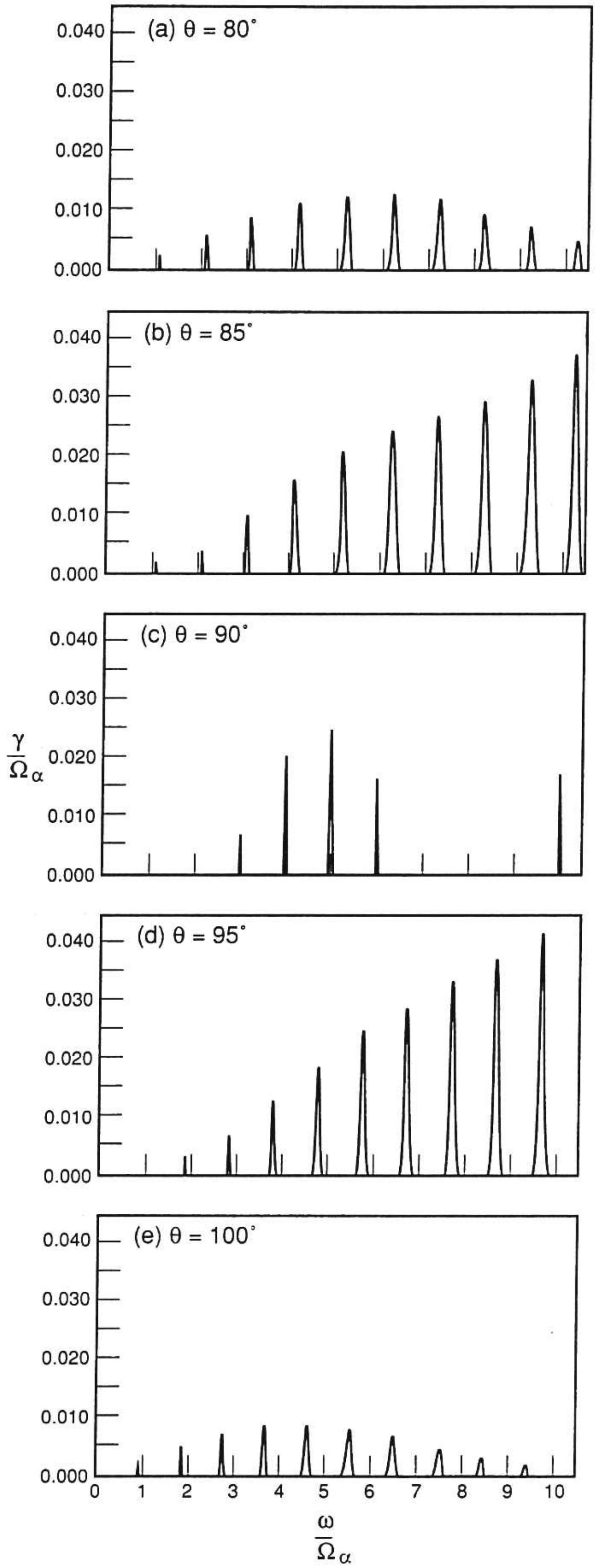
(a) θ = 80°
(b) θ = 85°
(c) θ = 90°
(d) θ = 95°
(e) θ = 100°
0.040
0.030
0.020
0.010
0.000
0 1 2 3 4 5 6 7 8 9 10
γ/Ω_α
ω/Ω_α

FIGURE 4

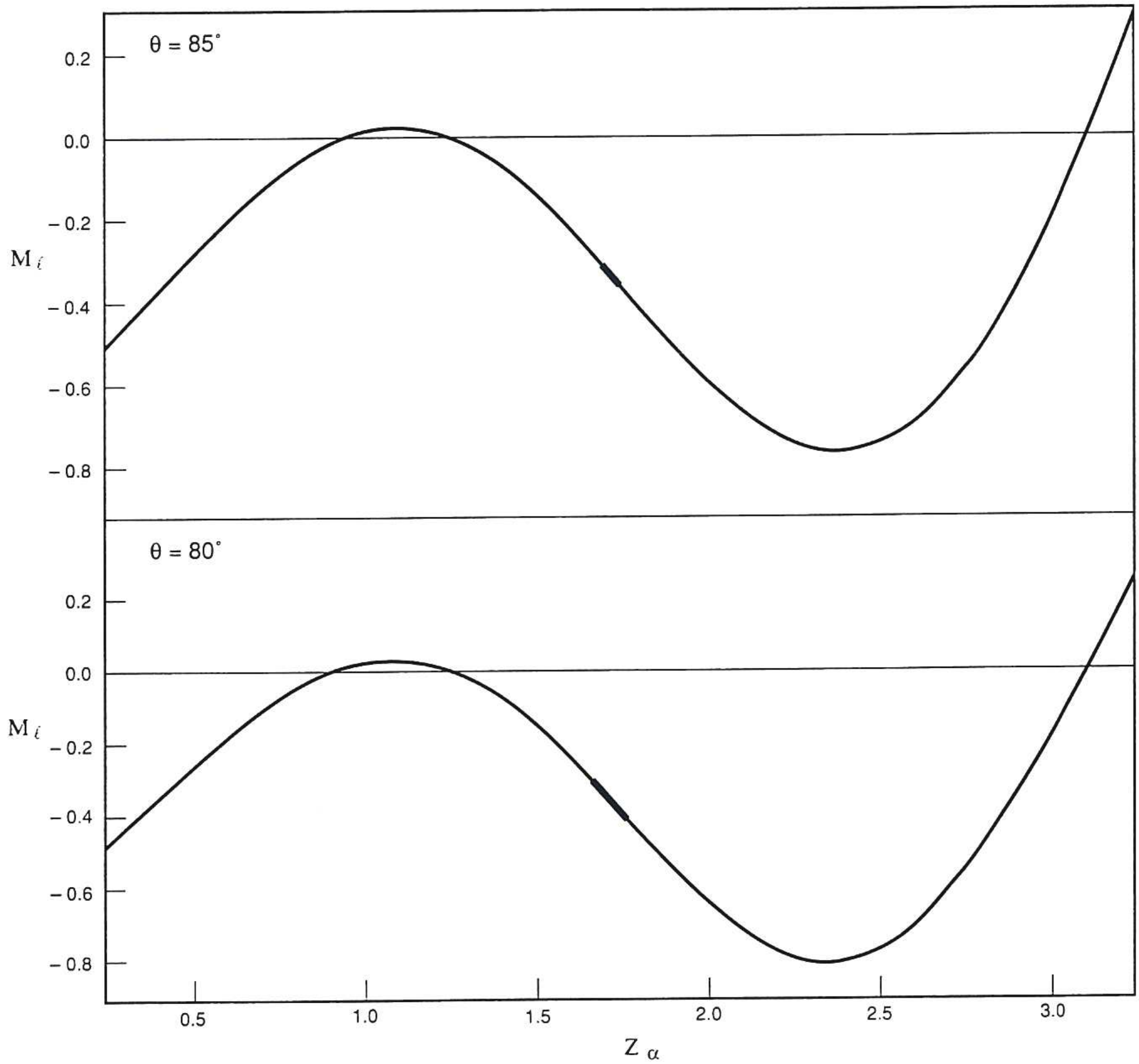

θ = 85°
0.2
0.0
− 0.2
M_i
− 0.4
− 0.6
− 0.8
θ = 80°
0.2
0.0
M_i
− 0.2
− 0.4
− 0.6
− 0.8
0.5
1.0
1.5
2.0
2.5
3.0
Z_α

FIGURE 5

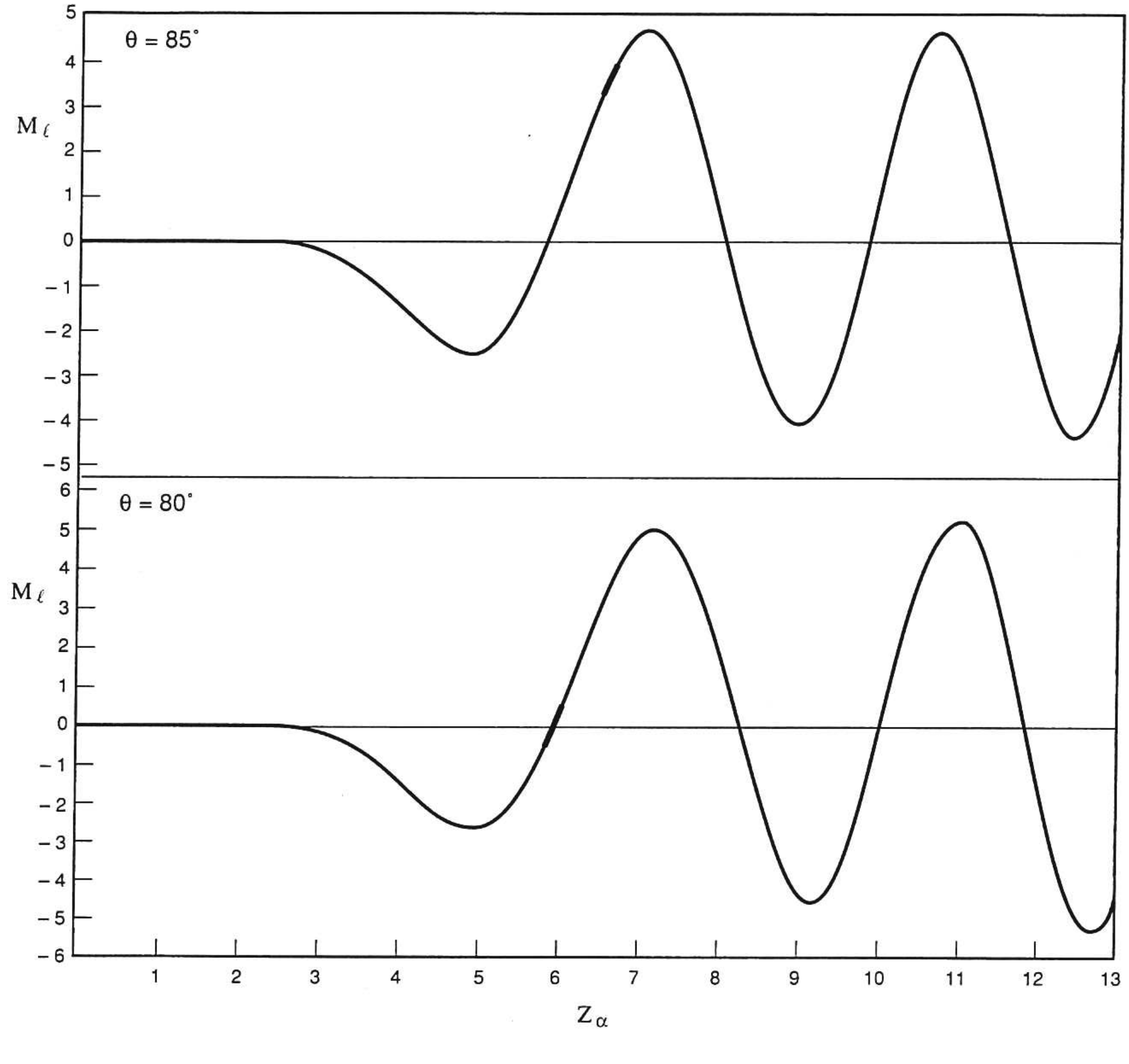
θ = 85˚
θ = 80˚
M ℓ
M ℓ
Z α
5
4
3
2
1
0
− 1
− 2
− 3
− 4
− 5
6
5
4
3
2
1
0
− 1
− 2
− 3
− 4
− 5
− 6
1
2
3
4
5
6
7
8
9
10
11
12
13